Permeability of self-affine aperture fields

Laurent Talon* and Harold Auradou†
Lab. FAST, Univ. Pierre et Marie Curie-Paris 6–Univ. Paris-Sud–CNRS, Bât. 502, Campus Univ., Orsay F-91405, France

Alex Hansen‡
Department of Physics, Norwegian University of Science and Technology, N-7491 Trondheim, Norway
(Received 9 April 2010; published 15 October 2010)

We introduce a model that allows for the prediction of the permeability of self-affine rough channels (one-dimensional fracture) and two-dimensional fractures over a wide range of apertures. In the lubrication approximation, the permeability shows three different scaling regimes. For fractures with a large mean aperture or an aperture small enough to the permeability being close to disappearing, the permeability scales as the cube of the aperture when the zero level of the aperture is set to coincide with the disappearance of the permeability. Between these two regimes, there is a third regime where the scaling is due to the self-affine roughness. For rough channels, the exponent is found to be $3-1/H$, where H is the Hurst exponent. For two-dimensional fractures, it is necessary to introduce an equivalent aperture b_c to make the scaling regime apparent. b_c is defined as the hydraulic aperture of the most restrictive barrier crossing the fracture normal to the flow direction. This regime is characterized by an exponent higher than that for the one-dimensional case: it is 2.25 for $H=0.8$ and 2.16 for $H=0.3$.

DOI: 10.1103/PhysRevE.82.046108 PACS number(s): 46.50.+a, 62.20.mt

I. INTRODUCTION

In the last decades important research efforts from different communities have been devoted to upscaling the permeability of fractures. One of the practical issues, for instance, for long-term sequestration or for geotechnical purposes, is to predict the behavior of the permeability under changing mechanical conditions [1]. To uncover fundamental physical properties of transport phenomena in fractures, laboratory tests on rock samples [2,3] or on modeled fractures [4] as well as numerical modeling [5] have been carried out. These studies have reported nontrivial relations between fracture aperture and the measured permeability. For large mean distance between the halves, the permeability is found to scale with the cube of this distance. In this limit, the fracture can be viewed as consisting of two parallel flat walls [3]. But, as soon as the halves are brought closer together, deviations from this cubic law due to the surface roughness are seen [6,7]. In the recent years, various theoretical models based on statistical averages, weak disorder perturbation expansions, or mean-field approximations have been tested to evaluate these deviations [8–16]. In spite of much invested work, most of the foregoing developments break down if contact zones exist in the fracture. When the fracture halves are brought even closer, all the fluid is finally forced to pass a single strait—or bottleneck—connecting the inlet and the outlet. Following the work of Ambegaokar, Halperin, and Langer (AHL) [17], the permeability of the entire fracture is then controlled by the permeability of the bottleneck [18,19]. When the fracture is further opened percolating channels arise. The permeability is not controlled anymore by the bottleneck since the flow may bypass this region. In a previous study, we have extended the bottleneck effect by introducing the concept of critical barrier or path [20]. In the present paper, we improve the method by taking into account secondary bottlenecks. Our approach allows us to identify three regimes: the AHL regime (close to percolation), the cubic law regime for large mean aperture, and an intermediate nonlinear regime where the permeability is controlled by the successive critical constrictions. In Sec. II, we derive an extension of the bottleneck concept for flow in one-dimensional (1D) rough channels. In Sec. III, we extend the critical path analysis to two-dimensional (2D) fractures. We assume an aperture field which is the free space between a flat and a rough surface of height $h(x,y)$. Hence, the aperture is defined as $h(x,y)+a$, where a is the aperture measured from the percolation point, i.e., for $a \leq 0$ there is no conducting channels, and the permeability is zero. As soon as $a>0$, there is permeability. Possible contacts between the surfaces are also considered, and flow is assumed to take place only in open voids of the fracture where $a(x,y)>0$. Places where the aperture is negative are considered in contact, and their corresponding aperture $h(x,y)+a$ is set to zero. The fracture aperture is changed by moving apart the mean planes of the two surfaces, and its permeability is then analytically (when the field is 1D) or numerically (for 2D fields) computed by assuming that the Reynolds equation holds locally. We note, however, that deviations from this law may be expected for small mean separation between the fracture walls [21].

In the present work, we consider aperture fields with self-affine correlations, which are known to characterize natural fractures [22–24]. Such aperture fields have a two-point function $p_2(\Delta h, \Delta \vec{r})$, giving the probability density to find a height difference Δh over a distance $\Delta \vec{r}$ that shows the invariance

$$\lambda^H p_2(\lambda^H \Delta h, \lambda \Delta \vec{r}) = p_2(\Delta h, \Delta \vec{r}), \quad (1)$$

*talon@fast.u-psud.fr
†auradou@fast.u-psud.fr
‡alex.hansen@ntnu.no

where H is the *Hurst* or *roughness* exponent and λ is an arbitrary scaling factor. In this work, self-affine surfaces (1D and 2D) are generated using a Fourier transform method.

II. ONE-DIMENSIONAL SYSTEMS

We start by considering one-dimensional flow. In this case, the fracture field is assumed invariant in the y direction, and the flow occurs through a rough channel with local aperture $h(x)+a$. The flow is totally stopped as soon as the two surfaces come into contact, leading here to $\min_x h(x)=0$. The permeability K of this one-dimensional aperture field is, in the lubrication limit, given by the integral

$$\frac{L}{K} = \int_{x_0}^{x_L} \frac{dx}{k(h(x)+a)^3}, \tag{2}$$

where k is a constant and $x_L - x_0 = L$ is the length of the system. When the rough profile is discretized over a length Δ, so that $h(x) \to h_k$, Eq. (2) becomes

$$\frac{L}{K} = \sum_0^{L/\Delta} \frac{\Delta}{k(h_k+a)^3}. \tag{3}$$

Before considering self-affine correlations in $h(x)$, we investigate the simpler but unrealistic case when there are no spatial correlations. This is done in order to introduce the concepts that will be central in the following.

A. Uncorrelated aperture fields

When the aperture field has no spatial correlations, we use order statistics combined with Eq. (2) to determine the scaling properties of the permeability. The aperture field is fully characterized by the probability density $p(h)$, and its cumulative probability is $P(h)=\int_0^h dh' p(h')$. By taking the advantage that in Eq. (2) the occurrence order of the apertures does not matter, we may therefore order the $h(x)$ distribution in ascending order. The ordering transformation is $h(x) \to h[\xi] = h(x[\xi])$, where $h[\xi_1] \le h[\xi_2]$ if $\xi_1 \le \xi_2$. We define $\bar{h}[\xi]$ as the average of $h[\xi]$ over an ensemble of realizations. From order statistics [25], we then have

$$P(\bar{h}[\xi]) = \frac{\xi}{L}. \tag{4}$$

Note that we have, by definition, $\bar{h}[0]=0$ and $\langle \max_{x\in[0,L]} h(x) \rangle = \bar{h}[L]$, where $\langle \cdots \rangle$ refers to an ensemble average. The average inverse permeability is then given by the expression

$$\frac{L}{K} = \int_0^L \frac{d\xi}{k(\bar{h}[\xi]+a)^3} = \int_0^L \frac{d\xi}{k(P^{-1}(\xi/L)+a)^3}, \tag{5}$$

In the situation where the aperture field is distributed according to a power law, $p(h) \propto h^{\alpha-1}$, where $\alpha > 0$, bounded above by δ, the cumulative probability is given by $P(h) = (h/\delta)^\alpha$. This leads to

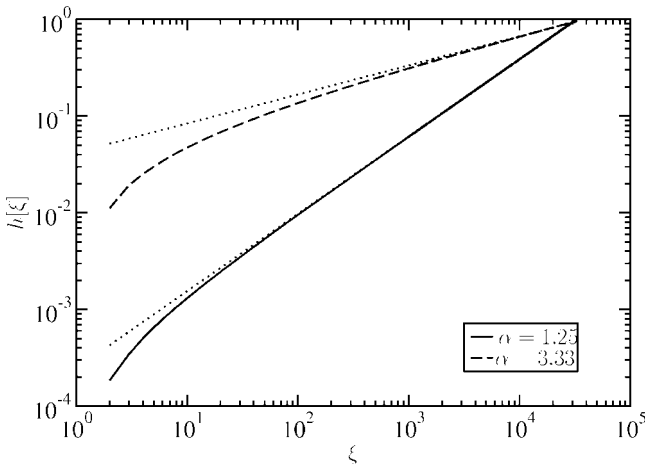

FIG. 1. Ordered sequences $h[\xi]$ from an uncorrelated noise distributed on the interval [0,1] according to the power law $p(h) \sim h^{\alpha-1}$ with exponents $\alpha=1.25$ (solid line) and 3.33 (dashed line). The data have been averaged over 1000 samples and each sample has a length of 2^{15}. The dotted lines have slopes of $0.8=1/1.25$ and $0.3=1/3.33$, respectively.

$$\bar{h}[\xi] = P^{-1}(\xi/L) = \frac{\delta}{L^{1/\alpha}} \xi^{1/\alpha}. \tag{6}$$

This result is illustrated in Fig. 1 where the ordered sequence $\bar{h}[\xi]$ is shown as a function of ξ for $\alpha=1.25$ and 3.33, respectively.

The permeability of a power-law-distributed aperture field is then given by the integral

$$\frac{L}{K} = \int_0^L \frac{d\xi}{k((\delta/L^{1/\alpha})\xi^{1/\alpha}+a)^3}. \tag{7}$$

We show in Fig. 2 the permeability K as a function of the

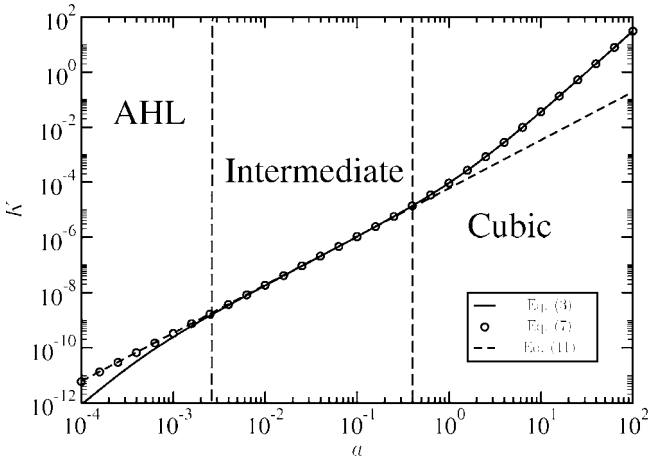

FIG. 2. Permeability K averaged over 1000 fields of length 2^{15} with h distributed according to a power law $p(h) \sim h^{\alpha-1}$ on the unit interval, where $\alpha=1.25$. Solid line and open circles show, respectively, the permeability K calculated from Eqs. (3) and (7) as a function of minimum opening a. The three scaling regimes are delimited by vertical lines. The dashed line represents $a^{3-\alpha}=a^{1.75}$.

opening a for $\alpha=1.25$ based on lubrication limit expression (3) together with the solution of Eq. (7).

As is apparent in Fig. 2, there are three power-law regimes. We identify them in the following. By introducing the notation

$$I(y) = \frac{1}{y^\alpha}\int_0^{y^\alpha} \frac{d\xi}{(\xi^{1/\alpha}+1)^3}, \tag{8}$$

Eq. (7) may be written as

$$\frac{1}{K} = \frac{I(\delta/a)}{ka^3}. \tag{9}$$

Depending on the value of the ratio a/δ, I displays two scaling regimes. In the first limit, when $a/\delta \to \infty$, corresponding, for instance, to a widely open fracture or to a fracture with small wall roughness, $I(\delta/a)$ tends to 1 and Eq. (9) becomes

$$K = ka^3. \tag{10}$$

In this regime, the permeability follows the classical cubic law. In the other limit, when $a/\delta \to 0$, i.e., when the fracture is closed, we deduce from Eq. (7) that the inverse permeability behaves as

$$\frac{1}{K} = \frac{I_\infty}{ka^3}\left(\frac{a}{\delta}\right)^\alpha \sim \frac{1}{a^{3-\alpha}}, \tag{11}$$

where

$$I_\infty = \int_0^\infty \frac{d\xi}{(\xi^{1/\alpha}+1)^3}. \tag{12}$$

When $\alpha=1.25$, $I_\infty \approx 0.520\,65$. Hence, in this regime, the permeability shows a nonlinear variation with the fracture aperture with an exponent $3-\alpha$.

The relation given by Eq. (11) breaks down for small enough a when the system is discretized, $h(x) \to h_k$. When discretized, Eq. (7) reads

$$\frac{L}{K} = \sum_0^{L/\Delta} \frac{\Delta}{k(W/(L/\Delta)^{1/\alpha}k^{1/\alpha}+a)^3}. \tag{13}$$

For small enough a, the first term in the sum will dominate, and the permeability is then given by

$$K = \frac{L}{\Delta}ka^3. \tag{14}$$

This third scaling regime is visible in Fig. 2 for the permeability calculated from discretized fields h_k, where $1 \le k \le 2^{15}$. The analytical calculation based on Eq. (7) (dashed line in Fig. 2) does not exhibit such a regime.

In this paragraph, we have demonstrated that for uncorrelated power-law-distributed aperture field three scaling regimes exist: for small a/δ, $K \sim a^3$; for intermediate a/δ, $K \sim a^{3-\alpha}$; and for large a/δ, $K \sim a^3$ again. The next section extends this feature to self-affine correlated fields.

B. Self-affine correlations in the aperture field

As in the previous case, the zero level of the self-affine field $h(x)$ is adjusted, so that $\min_x h(x)=0$. Because of correlations, Eq. (4) cannot be straightforwardly used to compute the permeability. Rather, the averaged ordered sequence of h is given by

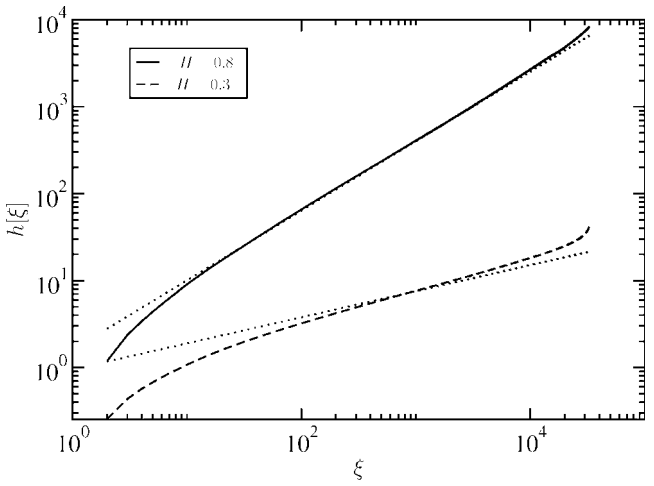

FIG. 3. Ordered and averaged sequence $\bar{h}[\xi]$ based on 1000 self-affine $h(x)$ with Hurst exponents equal to 0.8 and 0.3, respectively. The data consist of 1000 samples of length 2^{15}. The straight lines are $\xi^{0.8}$ and $\xi^{0.3}$, respectively.

$$\bar{h}[\xi] = c\xi^H, \tag{15}$$

where c is a prefactor. The reason for this is that since all moments of $h(x)$ taken at a distance x from the origin where we have $h(x=0)=0$ behave as

$$\langle |h(x)|^q \rangle^{1/q} \sim x^H, \tag{16}$$

we must have $\xi \propto x$ and Eq. (15) follows. We test Eq. (15) in Fig. 3. For H larger than 0.5, the scaling predicted by Eq. (15) falls onto the numerical observation, for ξ larger than 50 (similarly with the power-law distribution; see Fig. 1). However, for smaller values of H, the deviation becomes larger (see Fig. 3). For the 1D situation, we shall only consider a Hurst exponent $H>0.5$.

We now combine Eq. (15) with Eq. (5) to calculate the permeability,

$$\frac{L}{K} = \int_0^L \frac{d\xi}{k(c\xi^H+a)^3}. \tag{17}$$

We show in Fig. 4 the permeability derived from calculation of Eq. (3) and from Eq. (17).

Since Eqs. (17) and (7) are formally identical, the scaling analysis presented in Eqs. (8)–(10) is the same for the self-affine case as for the power-law-distributed and uncorrelated functions when the exponent α is substituted for $1/H$. Hence, for intermediate minimum apertures a, we find the scaling

$$K = \frac{k}{I_\infty}La^{3-1/H}. \tag{18}$$

We note that the permeability is in this intermediate regime proportional to the length L. This is different from the prediction of Roux *et al.* [26] giving $K \sim L^{3H}$ in the same

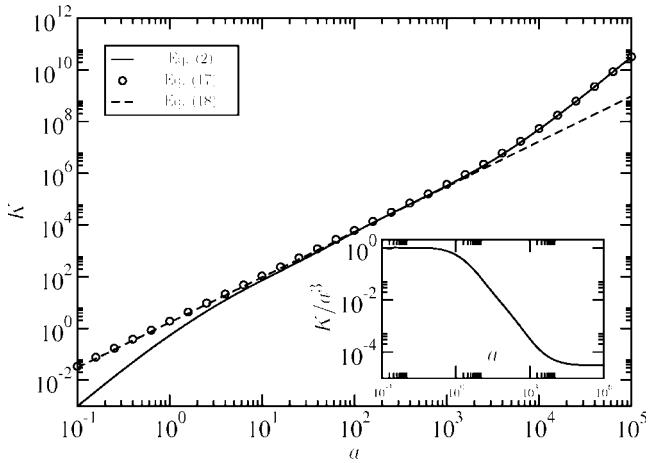

FIG. 4. Permeability K defined in Eq. (3) as a function of minimum opening a for 1000 self-affine fields $h(x)$ of length 2^{15} with $H=0.8$. We also show integral (17) as a function of a. The straight dotted line is the power law $a^{3-1/H}=a^{1.75}$ [Eq. (18)]. The inset shows the normalized permeability K/a^3.

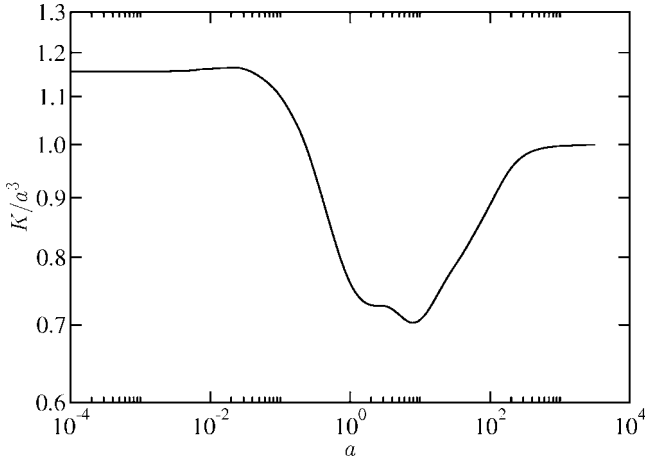

FIG. 5. Permeability K/a^3 as a function of opening a for 100 self-affine samples of size 1024. For small and large a's, $K\sim a^3$, but with different prefactors.

regime. This calculation was based on the assumption that $K\sim W^3$, where W is the average aperture when the fracture surfaces are close to contact. The self-affinity then gives $W\sim L^H$, and $K\sim L^{3H}$ follows. However, Eq. (18) shows that even though the fracture opening a is large enough, so that the $\min_x h(x)$ region no longer dominates, W does not enter the expression, and the permeability is proportional to L rather than L^{3H}.

For small enough a, the region around the minimum aperture dominates, and the permeability is given by Eq. (14). This was noted by Gutfraind and Hansen [27] in their numerical study based on lattice-gas automata.

III. TWO-DIMENSIONAL APERTURE FIELDS

In going from one to two dimensions, i.e., when the aperture field is a function of points in a plane (x,y) rather than only x, the concept of the narrowest constriction needs to be redefined. In one dimension, the narrowest constriction is the point along the fracture where there is first contact between the two halves. This definition does not work in two dimensions. The point at which there is first contact will have little influence in this case, as the flow simply goes around it; and, if the two halves are brought further into contact, deformation occurs. In this work, deformations are modeled as follows: the aperture field is defined by $u(x,y)=u+h(x,y)$. Contact points (and thus deformations) appear wherever $u(x,y)<0$. Hence, we model the deformation at those points by setting the aperture equal to zero as follows:

$$n(x,y)=\max_{(x,y)}[u(x,y),0]. \tag{19}$$

Hence, by replacing $h(x,y)+u$ with $n(x,y)$ we model in a simple way the possible overlaps of the walls.

In one dimension, the aperture of the narrowest constriction is a. When a approaches zero, the permeability decreases and reaches zero for $a=0$. We wish to define the aperture in the same way in two dimensions, namely, a is the aperture for which the permeability reaches zero. When the aperture is close to this value, the permeability is controlled by a single strait as argued in a different context by Ambegaokar *et al.* [17]. The minimum-maximum algorithm of Hansen *et al.* [28,29] is used to identify the position of this particular point. First, we identify the minimum height along each path connecting the inlet to the outlet. The highest of the minimum height gives then the minimal vertical shift for which flow occurs. We will denote by a this height. Note that, using this method, one can also localize the percolation point that according to Ambegaokar *et al.* [17] should control the permeability.

Figure 5 shows the permeability, computed by solving the Kirchhoff equations, as a function of the aperture a. The normalization of the permeability by a^3 highlights two plateaus for, respectively, small and large a's. They correspond to the two cubic regimes already observed in the one-dimensional case.

In the intermediate regime, however, the normalized permeability does not show a power law in contrast to the one-dimensional case (see the inset of Fig. 4). This hints that at the aperture a does not correspond to the aperture defined in the one-dimensional case. We now identify the proper variable for this. In a recent paper, Talon *et al.* [20] replaced the one-dimensional notion of the "narrowest constriction" with the "most restrictive path" in two dimensions. If $\mathcal{C}$ is one out of all the possible paths that cut across the sample between the two edges parallel to the average flow direction, we may assign an "effective permeability" to it as the integral of $n^3(x,y)$ along $\mathcal{C}$. We then identify the path with the *smallest* effective permeability,

$$b_c=\frac{1}{L}\left[\min_{\mathcal{C}}\int_{\mathcal{C}} d\vec{\ell}\cdot\vec{e}_\perp n^3(\vec{\ell})\right]^{1/3}, \tag{20}$$

where $\vec{e}_\perp$ is a unit vector pointing in the direction orthogonal to the average flow direction. When $a\ll 1$, b_c will essentially be equal to a, as the only opening along the most restrictive

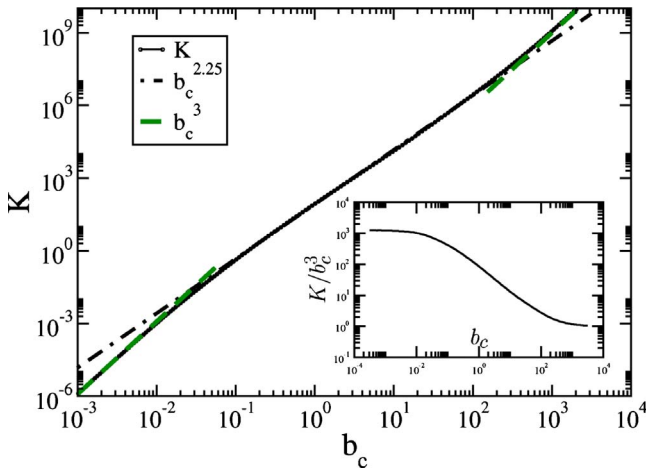

FIG. 6. (Color online) Permeability K as a function of b_c for 100 self-affine samples with $H=0.8$ of size 1024×1024. The straight lines are $b_c^{2.25}$ and b_c^3, respectively.

path will be the AHL strait. However, for larger values of a, they will no longer coincide. As a is increased even further, they again approach each other.

We show in Fig. 6 permeability K as a function of b_c as defined in Eq. (20). There are the small and large b_c regimes where $K\sim b_c^3$. However, now there is also an intermediate regime where there is power-law behavior,

$$K \sim b_c^{2.25\pm0.02}, \tag{21}$$

for $H=0.8$. For surfaces with $H=0.3$, we find an exponent 2.16 ± 0.02.

In order to understand where this intermediate power-law regime comes from, we generalize the concept of b_c. Assume now that we are no longer looking for the most restrictive path for the entire sample, but for other restrictive paths that start at a position x,

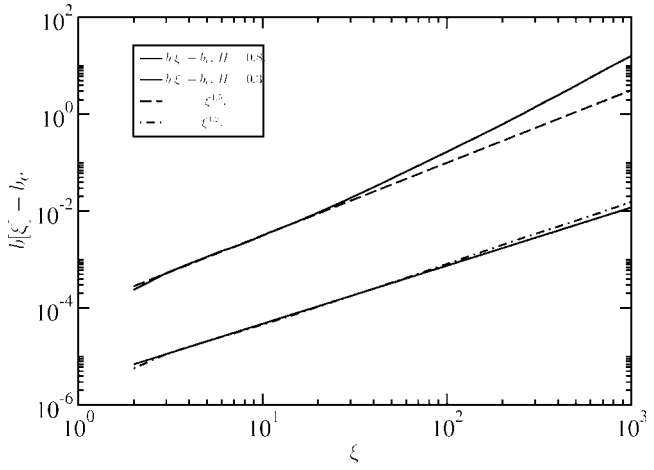

FIG. 7. Ordered sequences $b[\xi]-b_c$ from 1000 samples of size 1024×1024 with Hurst exponents $H=0.8$ and $H=0.3$, respectively. The straight lines are proportional to $\xi^{1.2}$ and $\xi^{1.5}$, respectively.

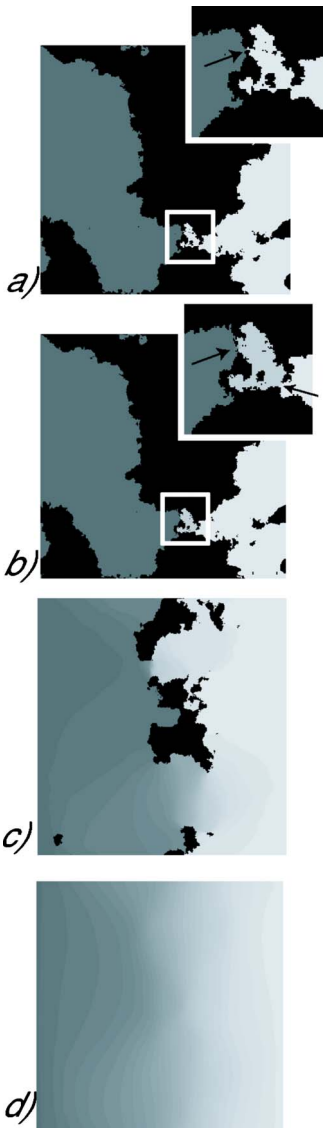

FIG. 8. (Color online) Pressure field in gray levels a self-affine realization. The flow is from left to right. Dark regions correspond to contact zones. From top to bottom: $(b-b_c)=10^{-4}$ (AHL regime, the arrow indicates the percolation point), 0.5 (crossover regime, the arrows show the two significant pressure drops corresponding to the two major barriers), 28 (crossover regime), and 97 (cubic law regime).

$$b(x) = \frac{1}{L}\left[\min_{\mathcal{C}(x)} \int_{\mathcal{C}} d\vec{\ell}\cdot\vec{e}_{\perp} n(\vec{\ell})^3\right]^{1/3}, \tag{22}$$

where $\mathcal{C}(x)$ is a path starting at x. In practice we use a transfer-matrix algorithm for this [30]. We have that the most restrictive path is given by $b_c=\min_x b(x)$.

We may now order the local most restrictive paths, $b(x)\to b[\xi]$. Figure 7 shows the ordering statistic of $b[\xi]-b_c$ obtained for self-affine surfaces $h(x,y)$. For ξ smaller than 50, $b[\xi]-b_c$ is found to follow a power law characterized by an exponent β close to 1.5 for $H=0.8$ and $\beta=1.2$, for $H=0.3$.

The local most restrictive path $b(x)$ plays the role of $a+h(x)$ in the one-dimensional case. Under this assumption, the two-dimensional permeability is given by

$$\frac{L}{K} = \int_0^L \frac{dx}{kb^3(x)} = \int_0^L \frac{dx}{k\{(b(x)-b_c)+b_c\}^3}. \quad (23)$$

This equation should be compared to Eq. (3) for the one-dimensional system. b_c in the present case plays the role of a, and $b(x)-b_c$ plays the role of $h(x)$. Following the logic that led to Eq. (7), we would expect the exponent of the power law of the intermediate regime to be $3-1/\beta$; hence, 2.33 for $H=0.8$ and 2.16 for $H=0.3$. Clearly, the assumption that $b(x)$ could replace $a+h(x)$ in an equivalent system does lead to a reasonable determination of the exponent.

The three regimes are qualitatively illustrated in Fig. 8 that shows the pressure field for different values of $(b-b_c)$. In Fig. 8(a), we see the regime for which the permeability is controlled by a single element—the AHL regime, giving rise to a cubic law behavior. Figures 8(b) and 8(c) show the crossover regime giving rise to the intermediate power law in the permeability. Figure 8(d) shows the large-opening regime where again a cubic law is found.

IV. SUMMARY AND DISCUSSION

We have in this paper discussed permeability of fractures as a function of fracture opening. We identify three regimes: a first regime where the permeability is completely controlled by one single local area. This area is that identified by the AHL construction and is closely related to the percolation point. In one-dimensional channels, it corresponds to the narrowest constriction. In this regime, we find that the permeability follows a cubic law with respect to the fracture opening. When the fracture opening is very large, another cubic law regime is found. The prefactors of the two cubic laws are different. Between these two regimes, there is an intermediate regime where nontrivial scaling is found. In one-dimensional systems, this scaling can be derived thanks to order statistics for uncorrelated power-law aperture distribution. In the case of self-affine aperture field, despite long-range correlations the order statistics also follows a power law as for the uncorrelated aperture field. Consequently, the three scaling regimes are observed for self-affine fractures, with an intermediate exponent of $3-1/H$.

However, in two dimensions, ordering the permeability distribution modifies the effective permeability; ordering statistics is thus no longer applicable in this form. We improved the approach proposed in a previous work [20] where we introduced the concept of most restrictive path. We used the same concept to model the fracture as a sequence of transverse barriers put in a series. The concept of a path defined here should *not* be confused with that of a flow path. A hydraulic aperture is then estimated for each barrier. The problem reduces then to a one-dimensional one, where ordering is allowed. We have then shown that the order of each most restrictive barrier displays a power-law trend. This model allows us to interpret three observed scaling regimes as functions of the equivalent aperture b_c of the most restrictive path. However, contrary to the one-dimensional case, the scaling law could not be predicted from the roughness of the fracture wall. The obtained exponent for 2D is higher than that for the 1D channel. This indicates that the deviation to the cubic law is less important in 2D systems. This can be understood from the bypass effect and the localization of the flow. Yet, our approach introduces a different scale b_c which allows us to continuously describe the crossover from the AHL regime to the "cubic law" one using a framework which is the same in one and two dimensions. To our knowledge none of the previous methods describe such a behavior.

The numerical simulations performed here are based on lubrication theory. This approximation may, however, fail to correctly estimate the flow field as soon as the roughness significantly varies over small distances. Future work with flow fields estimated by solving the three-dimensional Stokes equation will be carried out. Other permeability distributions will be considered to generalize our model. We also believe that an extension to three-dimensional permeability field is worth investigating.

ACKNOWLEDGMENTS

We thank J. P. Hulin for many interesting discussions. A.H. thanks the Université de Paris-Sud 11 for financial support. H.A. and L.T. thank the PICS "The Physics of Geological Complex System" and the Réseaux de Thématiques de Recherches Avancées "Triangle de la physique" for financial support.

[1] Committee on Fracture Characterization and Fluid Flow, *National Research Council Rock Fractures and Fluid Flow: Contemporary Understanding and Applications* (National Academies Press, Washington, D.C., 1996).
[2] K. G. Raven and J. E. Gale, Int. J. Rock Mech. Min. Sci. Geomech. Abstr. **22**, 251 (1985).
[3] P. A. Witherspoon, J. Y. Wang, K. Iway, and J. E. Gale, Water Resour. Res. **16**, 1016 (1980).
[4] Y. Méheust and J. Schmittbuhl, Geophys. Res. Lett. **27**, 2989 (2000).
[5] V. V. Mourzenko, O. Galamay, J. F. Thovert, and P. M. Adler, Phys. Rev. E **56**, 3167 (1997).
[6] P. A. Witherspoon, Geophys. Res. Lett. **8**, 659 (1981).
[7] V. V. Mourzenko, J.-F. Thovert, and P. M. Adler, Transp. Porous Media **45**, 89 (2001).
[8] S. R. Brown, Geophys. Res. Lett. **13**, 1430 (1986).
[9] S. R. Brown, J. Geophys. Res. **92**, 1337 (1987).
[10] S. R. Brown, J. Geophys. Res. **94**, 9429 (1989).
[11] R. W. Zimmerman and G. S. Bodvarson, Transp. Porous Media **23**, 1 (1996).
[12] J. Walsh, S. Brown, and W. Durham, J. Geophys. Res. **102**, 22587 (1997).

[13] G. Drazer and J. Koplik, Phys. Rev. E **66**, 026303 (2002).
[14] J. Inoue and H. Sugita, Water Resour. Res. **39**, 1202 (2003).
[15] H. Auradou, G. Drazer, J. P. Hulin, and J. Koplik, Water Resour. Res. **41**, W09423 (2005).
[16] W. Mallikamas and H. Rajaram, Geophys. Res. Lett. **32**, L11401 (2005).
[17] V. Ambegaokar, B. I. Halperin, and J. S. Langer, Phys. Rev. B **4**, 2612 (1971).
[18] A. J. Katz and A. H. Thompson, Phys. Rev. B **34**, 8179 (1986).
[19] L. J. Pyrak-Nolte, N. G. W. Cook, and D. D. Nolte, Geophys. Res. Lett. **15**, 1247 (1988).
[20] L. Talon, H. Auradou, and A. Hansen, Water Resour. Res. **46**, W07601 (2010).
[21] V. V. Mourzenko, J.-F. Thovert, and P. M. Adler, J. Phys. II **5**, 465 (1995).
[22] B. B. Mandelbrot, D. E. Passoja, and A. J. Paullay, Nature (London) **308**, 721 (1984).
[23] E. Bouchaud, G. Lapasset, and J. Planès, EPL **13**, 73 (1990).
[24] K. J. Måløy, A. Hansen, E. L. Hinrichsen, and S. Roux, Phys. Rev. Lett. **68**, 213 (1992).
[25] H. A. David and H. N. Nagaraja, *Order Statistics*, 3rd ed. (Wiley, New York, 2003).
[26] S. Roux, J. Schmittbuhl, J. P. Vilotte, and A. Hansen, EPL **23**, 277 (1993).
[27] R. Gutfraind and A. Hansen, Transp. Porous Media **18**, 131 (1995).
[28] A. Hansen and S. Roux, J. Phys. A **20**, L873 (1987).
[29] A. Hansen and E. L. Hinrichsen, Phys. Scr. **T44**, 55 (1992).
[30] A. L. Barabasi and H. E. Stanley, *Fractal Concepts in Surface Growth* (Cambridge University Press, Cambridge, England, 1995).